Supporting Information

Liin et al. 10.1073/pnas.1503488112

SI Materials and Methods

Molecular Biology. Expression plasmids human $K_V7.1$ (GenBank accession no. NM_000218) in pXOOM and KCNE1 (NM_000219) in pGEM have been previously described (1, 2). The truncation construct KCNE1ΔC was generated by introducing a stop codon at position 67 using mutated oligo extension PCR. The concatemers E1-$K_V7.1$-$K_V7.1$ and E1-$K_V7.1$ were kindly provided by R. S. Kass (Columbia University, New York, NY) and contained mutations to make the constructs suitable for voltage-clamp fluorometry recordings (3). Mutated cDNA was replaced by WT subunits by standard cloning techniques. All newly generated constructs were sequenced to ensure integrity (Genewiz). cRNA was prepared from linearized DNA using the T7 mMessage mMachine transcription kit (Ambion). RNA quality was checked by gel electrophoresis, and RNA concentrations were quantified by UV spectroscopy.

Experiments on *X. laevis* Oocytes. Experiments were performed 2 to 5 d after injection at room temperature with the two-electrode voltage-clamp technique (CA-1B Dagan amplifier). Currents were sampled at 1–3.3 kHz, filtered at 500 Hz, and not leakage corrected. The control solution contained (in mM) 88 NaCl, 1 KCl, 15 Hepes, 0.4 $CaCl_2$, and 0.8 $MgCl_2$ (pH adjusted to 7.4 using NaOH). Animal experiments were approved by the local ethics committees. The holding voltage was generally set to −80 mV, and activation curves by stepping to test voltages between −110 and +60 mV (2- to 4-s durations and 10-mV increments), followed by a tail voltage of −30 mV. For recordings of Kv7.1 at pH 9 and pH 10, the holding voltage was set to more negative voltages because the largest DHA-induced shifts induced channel opening already at −80 mV. In addition to effects on channel voltage dependence, arachidonyl amine induced Kv7.1 channel inactivation. Therefore, in arachidonyl amine experiments, a brief hyperpolarizing pulse of 50 ms to −120 mV was introduced between the test voltage and the tail voltage to relief the channels from inactivation.

Experiments on rat cardiomyocytes. On gestation day 16 of pregnancy, time-mated Sprague–Dawley rats (Taconic) were anesthetized in a CO_2 chamber followed by cervical dislocation. Cell preparation of cardiomyocytes and culturing on glass coverslips were made as previously described (4). Animal experiments were approved by the local ethics committees. Spontaneous action potentials and currents were measured using the patch-clamp technique in whole cell configuration 1–3 d after culturing. An Axopatch 200B patch-clamp amplifier, Digidata 1140A converter (Molecular Devices), and pClamp software (Molecular Devices) were used to acquire data. Data were recorded at 10 kHz and low-pass filtered at 2–5 kHz. For figures, currents were off-line filtered with a Gaussian filter, cutoff 200 Hz. The extracellular solution for action potential recordings contained (in mM) 140 NaCl, 5.4 KCl, 1 $MgCl_2$, 1.8 $CaCl_2$, 10 glucose, and 10 Hepes (pH 7.4, adjusted with NaOH). The intracellular solution contained (in mM) 130 K-gluconate, 9 KCl, 8 NaCl, 10 EGTA, 1 $MgCl_2$, 10 Hepes, and 3 MgATP (pH 7.3, adjusted with KOH). For current measurements, 1 μM E-4031 and 10 μM Nifedipine were added to the extracellular solution. The solutions were perfused through the recording chamber (flow: 0.5 mL/min). All experiments were carried out at 35 °C. All chemicals were purchased from Sigma-Aldrich. The patch pipettes, made of borosilicate glass, had a resistance between 4 and 6 MΩ once filled with intracellular solution. To analyze action potential characteristics, a stable 60-s recording was selected before and after application of the test solution. The average data

were then calculated for the complete trace in Clampfit 10 (Molecular Devices). To analyze the effect of Chromanol 293B on APD_{50}, the first 30 s of the trace after Chromanol 293B application was used. To analyze current amplitude, the holding voltage was set to −70 mV, and the steady-state current in the end of test pulses ranging from −70 to +40 mV was measured. Liquid junction potential was adjusted for in current measurements.

Isolated perfused heart preparations. Female guinea pigs (Dunkin Hartley, 450–600 g; Charles River) were anesthetized with sodium pentobarbital supplemented with lidocainhydrochloride (Sygehus Apotekerne). Upon thoracotomy, the aorta was cannulated to start a retrograde coronary perfusion with a modified Krebs'–Henseleit solution that contained (in mM) NaCl, 120.0; KCl, 4.0; $NaHCO_3$, 25.0; glucose, 11.0; $MgSO_4$, 0.6; KH_2PO_4, 0.6; and $CaCl_2$, 2.5. The solution was gassed with 95% O_2, 5% CO_2 and warmed (37 °C), to maintain pH at 7.4. Finally, the excised heart was mounted on a Langendorff-perfusion apparatus (Hugo Sachs-Harvard Apparatus) and perfused at a constant pressure of 60 mmHg. ECG signals were recorded using three ECG electrodes. A monophasic action potential electrode was placed on the right ventricle and a pacing electrode on the right atrium. Pacing periods consisted of 2-min pacing at 250 beats/min (BPM). All data were acquired at 2 kHz using a 16-channel PowerLab system (ADInstruments). The heart stabilized for a minimum of 30 min, followed by 2 min of pacing to record baseline electrocardiogram and APD_{90} at a constant heart rate. Next, the hERG/Kv11.1 inhibitor E4031 (0.03 μM) was added to the perfusate for 20 min, and data were acquired during 2-min atrial pacing. Finally 10 μM DHA-Gly was added to the perfusate, and the heart was paced for 2 min every 10th minute. All data are presented as the mean of the last 1-min recording during pacing. Drug effects on intrinsic heart rate were evaluated before initiation of pacing.

Test Compounds. 4,7,10,13,16,19-*all-cis*-Docosahexaenoic acid (DHA), 4,7,10,13,16,19-*all-cis*-docosahexaenoic acid methyl ester (DHA-me), 5,8,11,14,17-*all-cis*-eicosapentaenoic acid (EPA), and methyl 9-*cis*-octadecenoic acid (oleic acid) were purchased from Sigma-Aldrich. Docosahexaenoyl glycine and *N*-arachidonoyl taurine were purchased from Cayman Chemical. *N*-arachidonoyl taurine is a very strong acid and is expected to be always ionized when in solution. It is therefore referred to as being permanently charged. Synthesis of arachidonyl amine and docosahexaenoyl amine was performed as described in Fig. S8. Test compounds were dissolved in 99.5% ethanol to a concentration of 100 mM and diluted shortly before experiments as previously described (5, 6). We expect all test compound concentrations of 70 μM and lower to be below the critical micellar concentration in our experimental setting (5, 7). For the highest DHA concentration used, 210 μM, we cannot be sure that there is no micelle formation. If we have micelle formation at 210 μM DHA, the free DHA concentration will not be 210 μM, which may affect our concentration-response estimates in Figs. 1C and 2C and tend to overestimate the $c_{0.5}$. The estimates for $c_{0.5}$ should therefore be seen as an approximation. Control solution was added to the bath using an gravity-driven perfusion system. To avoid binding of test compounds to the perfusion system, test solutions were added manually with a glass Pasteur pipette. Previously, the effective concentration of fatty acids was determined to be 70% of the nominal concentration due to binding to the Perspex chamber (5). All fatty acid and fatty acid analog concentrations denoted are the estimated effective concentrations, i.e., 70% of the nominal concentration. Generally, the test compound effect was

poorly reversible. The PUFA effect could not be washed away with pure control solution. When adding 100 mg/L albumin during washing, the recovery was much improved; however, it was not complete.

To avoid possible cyclooxygenase enzyme metabolization of arachidonyl amine and N-arachidonoyl taurine, oocytes were pretreated with 1 μM indomethacin, and 1 μM indomethacin was supplemented in the recording solutions as previously described (5).

Electrophysiological Analysis. To quantify effects on the voltage dependence, tail currents (measured shortly after initiation of repolarization) were plotted against the prepulse (test) voltage. The following Boltzmann relation was fitted to the control curve, and the given slope factor was noted

$$G(V) = A \big/ \left\{ 1 + \exp\left[\left(V_{1/2} - V \right) \big/ s \right] \right\}, \qquad \textbf{[S1]}$$

where $V_{1/2}$ is the midpoint and s the slope factor. The same Boltzmann relation was fitted to the test substance I_{tail} vs. voltage curve with the slope factor constrained to the value given for the control curve. The $V_{1/2}$ values were compared with quantify the shift in voltage dependence. For illustrative clarity in figures showing I_{tail} vs. voltage, the curves are normalized between 0 and 1. The curves shown in the figures are not Boltzmann fits but simply lines connecting the data points. Due to the slow activation kinetics of the Kv7.1/KCNE1 channel, the currents do not

always reach steady state in the experiments for the $G(V)$ curves (e.g., Fig. 3 A and C).

To quantify the concentration dependence and pH dependence of the DHA-induced shift of voltage dependence, ΔV, the following equation was used:

$$\Delta V = \Delta V_{max} / [1 + (c_{0.5}/c)], \qquad \textbf{[S2]}$$

where ΔV_{max} is the maximal shift, $c_{0.5}$ is the concentration causing 50% of the maximal shift, and c is the concentration of DHA (or H^+).

Statistical Analysis. Average values are expressed as means ± SEM. Mean values for shifts in voltage dependence were analyzed using a two-tailed one-sample t test, where mean values were compared with a hypothetical value of 0 or where mean values were compared with each other. Comparison of PUFA potency on VSD mutants was done by one-way ANOVA comparing the PUFA effect on each mutant with the PUFA effect on Kv7.1 WT (Dunnett's multiple comparison test). Effects of N-AT and chromanol 293B on embryonic rat cardiomyocytes were analyzed using a paired two-tailed t test. Effects of E4031 and DHA-Gly on whole guinea pig hearts were analyzed using one-way ANOVA with Turkey's multiple comparison test. $P <$ 0.05 is considered statistically significant.

1. Jespersen T, Grunnet M, Angelo K, Klaerke DA, Olesen SP (2002) Dual-function vector for protein expression in both mammalian cells and Xenopus laevis oocytes. *Biotechniques* 32(3):536–538, 540.
2. Schmitt N, et al. (2007) The novel C-terminal KCNQ1 mutation M520R alters protein trafficking. *Biochem Biophys Res Commun* 358(1):304–310.
3. Wang W, Xia J, Kass RS (1998) MinK-KvLQT1 fusion proteins, evidence for multiple stoichiometries of the assembled IsK channel. *J Biol Chem* 273(51):34069–34074.
4. Danielsson C, et al. (2013) Exploration of human, rat, and rabbit embryonic cardiomyocytes suggests K-channel block as a common teratogenic mechanism. *Cardiovasc Res* 97(1):23–32.

5. Börjesson SI, Hammarström S, Elinder F (2008) Lipoelectric modification of ion channel voltage gating by polyunsaturated fatty acids. *Biophys J* 95(5):2242–2253.
6. Börjesson SI, Parkkari T, Hammarström S, Elinder F (2010) Electrostatic tuning of cellular excitability. *Biophys J* 98(3):396–403.
7. Serth J, Lautwein A, Frech M, Wittinghofer A, Pingoud A (1991) The inhibition of the GTPase activating protein-Ha-ras interaction by acidic lipids is due to physical association of the C-terminal domain of the GTPase activating protein with micellar structures. *EMBO J* 10(6):1325–1330.
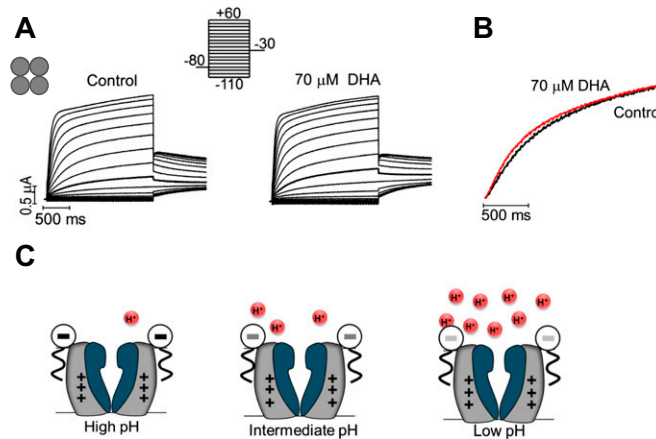
Fig. S1. DHA shifts the voltage dependence of Kv7.1. (*A*) Representative current families for the same cell as in Fig. 1*A* for control and 70 μM DHA on Kv7.1 channels. Currents for −20 mV are shown as bold traces. (*B*) Normalized current traces for −20 mV from a holding voltage of −80 mV. (*C*) Schematic illustration of pH dependence of PUFA protonation. The probability of protonation of the PUFA is indicated by the gray scale of the (−): dark gray, low probability of being protonated; light gray, high probability of being protonated.

Fig. S2. DHA methyl ester and DHA coapplication reduces the DHA effect on Kv7.1. (*A* and *B*) The $G(V)$ shift induced by 70 μM DHA on a representative cell when DHA is applied alone (*A*) or together with 70 μM DHA methyl ester (*B*; DHA-me). DHA or DHA+DHA-me (●), control (○). The dashed line in *A* is the control curve shifted −11 mV, and the dashed line in *B* is the control curve shifted −5.5 mV. (*C*) The same concentration-response curve as in Fig. 1*C* with experimental data for coapplication added (red circle). Means ± SEM; $n = 4$. The vertical arrow denotes the predicted $G(V)$ shift by 35 μM DHA deduced from the concentration-response curve.
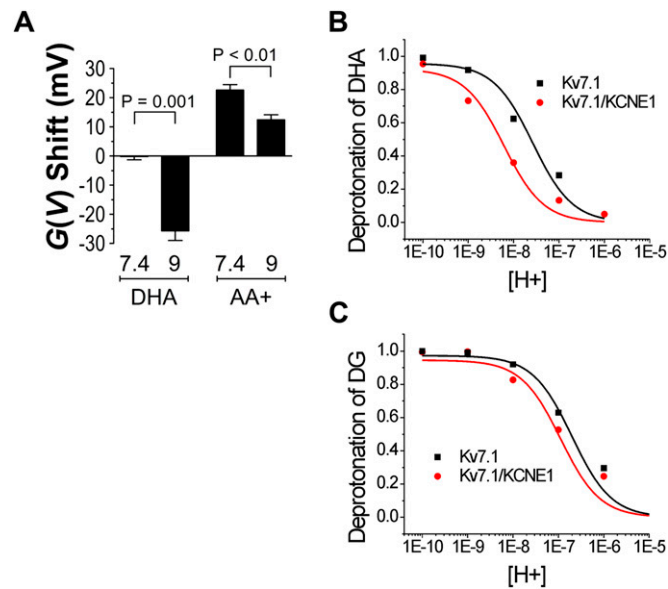

Fig. S3. DHA has no effect on Kv7.1/KCNE1ΔC and 2:4 and 4:4 Kv7.1:KCNE1 concatemers. (*A*) Kv7.1/KCNE1ΔC channel is insensitive to 70 μM DHA despite channel kinetics and voltage dependence being more similar to Kv7.1. DHA (●), control (○). Currents for −30 mV are shown as bold traces. (*B*) DHA (70 μM) induces a small shift in positive direction along the voltage axis for KCNE1-Kv7.1-Kv7.1 (forcing 4:2 Kv7.1:KCNE1 stoichiometry). DHA (●), control (○). Currents for 0 mV are shown as bold traces. The dashed line in *B* is the control curve shifted +7 mV. (*C*) DHA (70 μM) induces a small shift in positive direction along the voltage axis also in KCNE1-Kv7.1 (forcing 4:4 Kv7.1:KCNE1 stoichiometry) channel voltage dependence. DHA (●), control (○). Currents for +10 mV are shown as bold traces. The dashed line in *C* is the control curve shifted +5.5 mV.

Fig. S4. Arachidonoyl amine (AA+), DHA-Gly, and *N*-arachidonoyl taurine (*N*-AT) shift the voltage dependence of activation of Kv7.1/KCNE1. (*A*) AA+ (70 μM) at pH 7.4 induces a large shift in positive direction along the voltage axis in Kv7.1/KCNE1. AA+ (●), control (○). Currents for +20 mV are shown as bold traces. The dashed line in the right graph is the control curve shifted +28 mV. Note that the *G*(*V*) curves are from the same cell and not normalized. The continuous lines are Boltzmann curves (Eq. **1**) fitted to experimental data. The slope for AA+ is fixed to the same slope as for the control recording. (*B*) Representative current families for the same cell as in Fig. 4*A* for control and 70 μM DHA-Gly on Kv7.1/ KCNE1 channels. Currents for −20 mV are shown as bold traces. *G*(*V*) curve (same as in Fig. 4*A*) shown for comparison. (*C*) Representative current families for the same cell as in Fig. 4*C* for control and 70 μM *N*-AT on Kv7.1/ KCNE1 channels. Currents for 0 mV are shown as bold traces. *G*(*V*) curve (same as in Fig. 4*C*) shown for comparison.

Fig. S5. pH dependence PUFA analogs. (*A*) pH dependence of the DHA and AA+ effect on Kv7.1/KCNE1. $G(V)$ shift induced by 70 μM DHA or AA+ at pH 7.4 or pH 9. Data expressed as means ± SEM $n = 3–10$. (*B* and *C*) Model of pH dependence of the DHA and DHA-Gly effect on Kv7.1 and Kv7.1/KCNE1. The protonation state of DHA and DHA-glycine (DG) was calculated from the electroneutrality equation: $\Sigma(z_i[\text{ion}_i]_{\text{local}}) + z_{\text{PUFA}} [1 - 1/(1 + K_{\text{PUFA}}/[H^+]_{\text{local}})] + z_{\text{KCNE1}} [1 - 1/(1 + K_{\text{KCNE1}}/[H^+]_{\text{local}})] = 0$. Each local ion concentration was estimated using $[\text{ion}_i]_{\text{local}} = [\text{ion}_i] \exp(-z_i F V/kT)$. We assume that KCNE1 introduces extra negative charge with a pK_a of 7.7 in the microenvironment of the DHA compounds. We assume DHA has a pK_a of 7.7 in the microenvironment of Kv7.1 in the lipid bilayer in the absence of KCNE1. (*B*) pH dependence of protonation of DHA. Kv7.1: $c_{0.5} = 2 \times 10^{-8}$ = pH 7.7; Kv7.1/KCNE1: $c_{0.5} = 5 \times 10^{-9}$ = pH 8.3. (*C*) pH dependence of protonation of DHA-glycine. Kv7.1: $c_{0.5} = 1.9 \times 10^{-7}$ = pH 6.7; Kv7.1/KCNE1: $c_{0.5} = 1.4 \times 10^{-7}$ = pH 6.8.
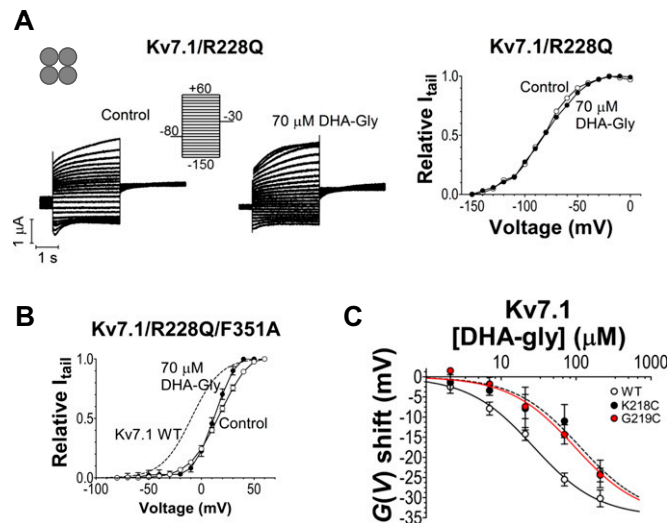

Fig. S6. VSD mutants reduce the effect of DHA-Gly on Kv7.1. (*A*) Representative current families for control and 70 μM DHA-Gly on Kv7.1/R228Q channels. (*B*) Voltage dependence of Kv7.1/R228Q/F351A and effect of 70 μM DHA-Gly. Means ± SEM; $n = 8$. Dashed line indicates Kv7.1 WT. (*C*) Concentration-response curves for the effect of DHA-Gly on Kv7.1, Kv7.1/K218C, and Kv7.1/G219C. ΔV_{max} was restricted to a shared value (−34.7 mV) to make the fits more robust. Kv7.1: $c_{0.5} = 27$ μM; Kv7.1/K218C: $c_{0.5} = 113$ μM; Kv7.1/G219C: $c_{0.5} = 96$ μM. Means ± SEM; $n = 3–14$.
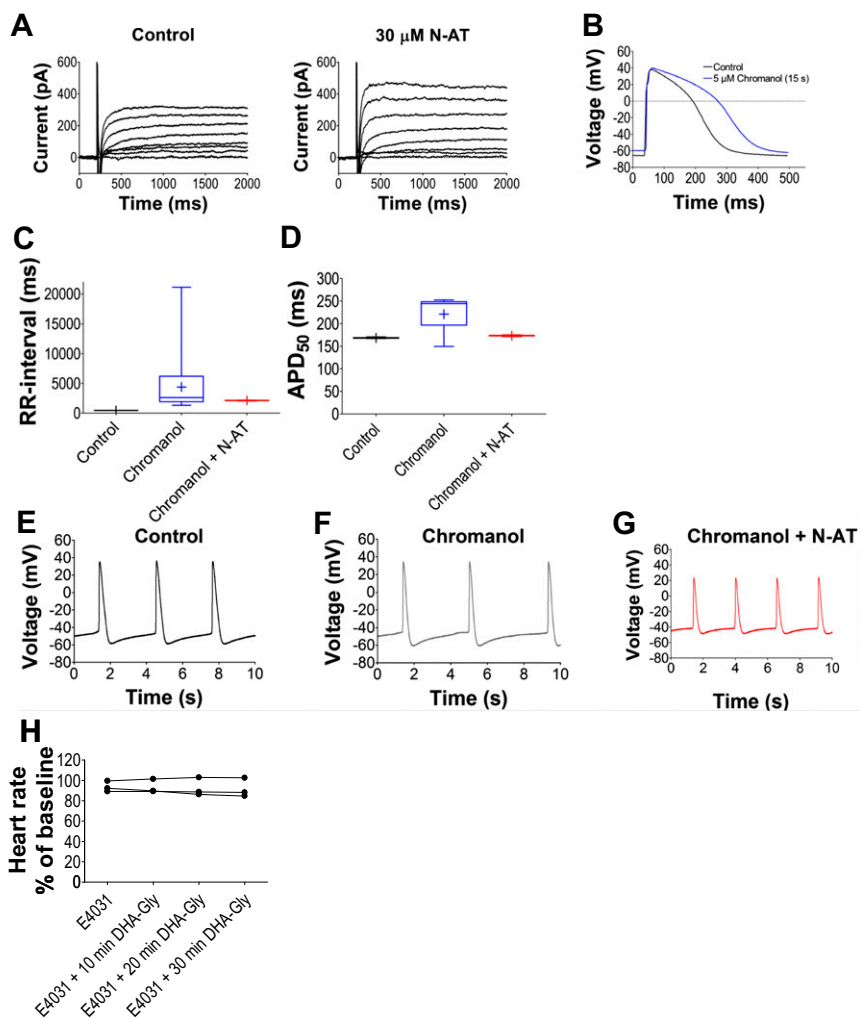
Fig. S7. Compound effect on embryonic rat cardiomyocytes and guinea pig heart. (*A*) Example of current in isolated embryonic rat cardiomyocytes before (*Left*) and after (*Right*) 30 μM *N*-AT application. E4031 and Nifedipine added. $V_{holding} = -70$ mV; test voltages = −70 to +20 mV. (*B*) Example of effect of 5 μM Chromanol 293B on action potential duration in one isolated embryonic rat cardiomyocyte. (*C* and *D*) Example of box plot plot for 5 μM Chromanol 293B effect on rhythmicity of spontaneous cardiomyocyte firing (*C*) and variability of action potential duration (*D*) in one isolated embryonic rat cardiomyocyte. Box = 25th to 75th percentile; horizontal line = median; plus sign = mean; whiskers = range. (*E–G*) Representative example of slowed firing induced by application of 5 μM Chromanol 293B or 5 μM Chromanol 293B + 30 μM *N*-arachidonoyl taurine (*N*-AT) in isolated embryonic rat cardiomyocytes. (*H*) Summary of effect of E4031 (0.03 μM) and DHA-Gly (10 μM) on intrinsic heart rate in three isolated perfused guinea pig hearts. Data normalized to baseline (control).
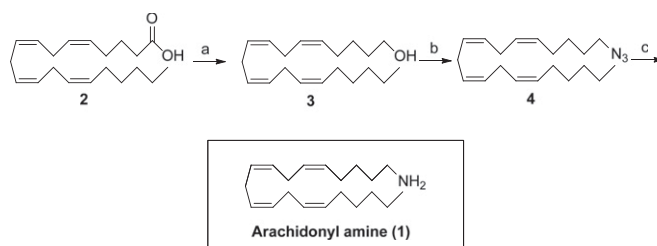

Fig. S8. Synthesis of arachidonyl amine. Synthesis of arachidonyl amine was performed essentially as previously described (6). As an exception to the previous synthesis description, arachidonic acid (2; Nu Chek Prep) was used as a starting material to produce arachidonyl alcohol (3). For synthesis of arachidonyl alcohol (3), LiAlH$_4$ (0.5 g, 13 mmol) was suspended into dry tetrahydrofuran (THF, 50 mL), and the mixture was cooled on an ice bath. Arachidonic acid (1.1 g, 3.5 mmol) in dry THF (40 mL) was added slowly. After the addition, stirring was continued for 1 h on the ice bath and an additional hour at room temperature. Ice cold water (1 mL) following 10% NaOH (0.2 mL) was added slowly, and stirring was continued for 1 h. The mixture was filtered through Celite, and the filtrate was dried over Na$_2$SO$_4$. Evaporation of solvents gave 800 mg (80%) of a colorless, oily product. ^{1}HNMR (CDCl$_3$): δ 0.89 (t, ^3J = 3.6 Hz, 3H), 1.19 (t, ^3J = 2.5 Hz, 1H) 1.25–1.39 (m, 6H), 1.42–1.48 (m, 2H), 1.57–1.62 (m, 2H), 2.04–2.13 (m, 4H), 2.80–2.85 (m, 6H), 3.66 (q, ^3J = 6.0 Hz, 2H), 5.31–5.43 (m, 8H). (a) 1. LiAlH$_4$, THF, 2. H$_2$O, 10% NaOH; (b) pyridine, methanesulphonyl chloride, 2. DMF, NaN$_3$; (c) LiAlH$_4$, THF, diethyl ether. Docosahexaenoyl amine was synthesized according to the same scheme but starting with docosahexaenoic acid.

Table S1. Effect of PUFAs and PUFA analogs on channel voltage dependence

Subunit stoichiometry	Construct	Compound	pH	$\Delta V_{1/2} \pm$ SEM (mV)	n	P*
	Kv7.1	70 µM DHA	7.4	−9.3 ± 0.9	3	<0.01
	Kv7.1	70 µM DHA	9.0	−25.1 ± 4.2	5	<0.01
	Kv7.1	70 µM EPA	7.4	−12.7 ± 1.4	3	0.01
	Kv7.1	70 µM OA	7.4	−1.0 ± 0.5	3	>0.1
	Kv7.1	70 µM DHA-me	7.4	+2.8 ± 2.5	3	>0.1
	Kv7.1	70 µM AA+	7.4	+9.7 ± 2.1	8	<0.01
	Kv7.1	70 µM DHA+	7.4	+7.8 ± 3.0	8	<0.05
	Kv7.1	70 µM DHA-Gly	7.4	−25.5 ± 1.6	14	<0.001
	Kv7.1	70 µM N-AT	7.4	−26.2 ± 2.7	4	<0.01
	Kv7.1/K218C	70 µM DHA-Gly	7.4	−11.0 ± 4.5	5	0.05
	Kv7.1/G219C	70 µM DHA-Gly	7.4	−14.3 ± 2.4	10	<0.001
	Kv7.1/R228Q	70 µM DHA-Gly	7.4	−0.6 ± 1.2	4	>0.5
	Kv7.1/E1	70 µM DHA	7.4	−0.2 ± 1.1	3	>0.5
	Kv7.1/E1	70 µM DHA	9.0	−25.7 ± 3.3	4	<0.01
	Kv7.1/E1	70 µM AA+	7.4	+22.6 ± 1.9	10	<0.0001
	Kv7.1/E1	70 µM DHA-Gly	7.4	−25.1 ± 3.9	6	0.001
	Kv7.1/E1	70 µM N-AT	7.4	−27.0 ± 2.5	5	<0.001
	Kv7.1/E1ΔC	70 µM DHA	7.4	−1.0 ± 1.7	8	>0.5
	E1-Kv7.1	70 µM DHA	7.4	+5.9 ± 1.4	15	<0.001
	E1-Kv7.1	70 µM DHA	9.0	−27.9 ± 4.7	6	<0.01
	E1-Kv7.1	70 µM DHA-me	7.4	+5.0 ± 1.3	5	<0.05
	E1-Kv7.1	70 µM DHA-me	9.0	+3.6 ± 2.6	4	>0.1
	E1-Kv7.1-Kv7.1	70 µM DHA	7.4	+5.0 ± 1.9	13	<0.05
	E1-Kv7.1-Kv7.1	70 µM DHA	9.0	−30.4 ± 2.5	6	<0.0001
	E1-Kv7.1-Kv7.1	70 µM DHA-me	7.4	+5.7 ± 0.9	6	<0.01
	E1-Kv7.1-Kv7.1	70 µM DHA-me	9.0	+8.2 ± 2.7	3	0.1

AA+, arachidonyl amine; DHA, docosahexaenoic acid; DHA-Gly, docosahaenoyl glycine; DHA-me, docosa-hexaenoic acid methyl ester; DHA+, docosahexaenyl amine; EPA, eicosapentaenoic acid; N-AT, N-arachidonoyl taurine; OA, oleic acid.
*From two-tailed one-sample t test where mean values were compared with 0.

Table S2. Summary of the effect of 30 µM N-AT on embryonic rat cardiomyocytes

Parameter	Control mean ± SEM	N-AT mean ± SEM	Change mean ± SEM	P	n
APD_{30}	261 ± 50 ms	211 ± 37 ms	−19 ± 4%	<0.05*	5
APD_{50}	341 ± 62 ms	279 ± 47 ms	−17 ± 3%	<0.05*	5
APD_{70}	402 ± 65 ms	336 ± 50 ms	−16 ± 3%	<0.05*	5
RR interval	2,869 ± 319 ms	2,075 ± 197 ms	−26 ± 5%	<0.05*	5
$Ampl_{peak}$	41 ± 3 mV	32 ± 2 mV	−9 ± 1 mV	<0.01*	5
RMP	−58 ± 2 mV	−56 ± 2 mV	+2 ± 1 mV	>0.1*	5

$Ampl_{peak}$, peak action potential amplitude; APD, action potential duration; N-AT, N-arachidonoyl taurine; RMP, resting membrane potential; RR interval, the inverse of action potential frequency.
*From two-tailed paired t test.